Electronic Supplementary Information

Guest Modulating the Photoactivity of a Titanium-Oxide Cage†

Dexin Wang,‡[a] Yanshu Liu,‡[a] Guanyun Zhang,*[a] Menghui Chu,[a] Fangfang Gao,[a] Guanjie Chen,[a] Guo Wang,[b] Chen-Ho Tung[a] and Yifeng Wang*[a]

[a] Key Laboratory for Colloid and Interface Science of the Ministry of Education, School of Chemistry and Chemical Engineering, Shandong University, Jinan 250100, China

[b] Department of Chemistry, Capital Normal University, Beijing 100048, China

D. Wang and Y. Liu have equally contributed to this work.

*Corresponding author email: guanyzhang@sdu.edu.cn, yifeng@sdu.edu.cn

1. Experimental Section

Materials

Titanium isopropoxide ($Ti(O^iPr)_4$, 98%) was purchased from Sigma-Aldrich Co. 3, 5-dibromosalicylic acid, salicylic acid (SA, 99.5%), P25 TiO_2 (80% anatase and 20% rutile, average particle size 25nm, BET surface area ≈ 50 $m^2\ g^{-1}$), epoxides, biphenyl (≥99%), tetra-*n*-butylammonium hexafluorophosphate ($TBAPF_6$, 98%), ferrocene (98%), tetrabutylammonium bromide (TBAB, 99%), cesium acetate (CsAc, 99%), and formic acid (85%) were purchased from Aladdin. These chemicals are analytical grade and were used without purification. $Ti_8O_8Bz_{16}$ (abbreviated as Ti_8) was synthesized following the literature method.[1] All solvents are analytical grade and were dried overnight with 5Å molecular sieve before use.

Characterizations

Single-crystal X-ray diffraction (SCXRD) data were collected on a Rigaku Oxford Diffraction XtaLAB Synergy diffractometer, which is outfitted with a HyPix-6000HE Hybrid Photon Counting detector operating in shutterless mode and an Oxford Cryosystems 800 Plus Cu Kα (λ = 1.54184 Å) radiation from a PhotonJet microfocus X-ray Source. Data were collected at 173 K, processed with the CrystAlisPro software suite, and solved/refined with ShelXS and ShelXL programs, included in the Olex2 1.3 software interface.[2] Appropriate restraints were applied to the geometries. Hydrogen atoms at the carbon atoms were placed in the calculated positions and refined isotropically with the riding model. The solvent mask was conducted using the Olex2 implementation of BYPASS. FTIR spectra were collected using a PerkinElmer Spectrum Two IR Spectrometer over the 400−4000 cm^{-1} range. UV-vis diffuse reflectance spectra (UV−vis DRS) were collected using an Ocean Insight USB2000+ miniature spectrometer and the reflectance standard $BaSO_4$. Raman spectra were obtained using a 532 nm laser on a QEPro high-performance Raman spectrometer (Ocean Insight). Electron paramagnetic resonance (EPR) spectra were acquired using JOEL X320 equipment. FLASH EA1112 elemental analyzer was used to perform elemental analyses (C and H). The Ti(IV) content was quantified using a colorimetric approach based on the UV-vis absorption of the yellow pertitanic acid complex of Ti(IV) and H_2O_2 produced in an acid-aqueous solution. $K_2TiO(C_2O_4)\cdot 2H_2O$ was used as an external standard. The details were reported previously.[3] Electrochemistry was studied using a CHI 660E potentiostat/galvanostat. The Horiba FluoroMax−4 spectrometer was used to obtain steady−state photoluminescence (PL) spectra. Time−resolved fluorescence decay spectra were measured using a time−correlated single−photon counting (TCSPC) method on an Edinburgh Fluorescence Measurement System FLS920. A 300-W Xenon lamp with a sunlight filter (Beijing China Education Au-light Technology Co., Ltd; light intensity ≈ 132 mW cm^{-2}) was used as the sunlight simulator. The cycloaddition reactions were monitored using a gas chromatograph (GC; Fuli Instruments, 9720 Plus). The powder X−ray diffraction (PXRD) patterns were collected using Rigaku SmartLab 9KW in situ X−ray diffraction. NMR spectra were measured using an Avance−500 MHz NMR spectrometer (Bruker, Switzerland) at room temperature. ^{133}Cs NMR was determined using cesium chloride as internal standard and D_2O as solvent. Focused ion beam scanning electron microscopy (FIB-SEM) micrographs were acquired using a Helios 5 CX scanning electron microscope operated at 15 kV.

Synthesis

Synthesis of $(NH_4)_2Ti_{14}O_{12}(Sal)_{10}(HSal)_{14}(C_3H_6O)_2\cdot 2(CH_3CN)\cdot 6(C_3H_6O)$ (denoted as $Ti_{14}(NH_4)_2$)

Salicylic acid (1.65 g, 12 mmol) and ammonium iodide (0.145 g, 1 mmol) were added to a 20 mL vial containing 4.0 mL of an acetonitrile and acetone (1:1 v/v) mixture. During the stirring, triethylenetetramine (5 drops), formic acid (15 drops, 0.3 mL), and $Ti(O^iPr)_4$ (0.92 mL, 3 mmol) were added dropwise to afford a red clarified solution. After stirring for an hour, the vials were sealed and heated in an 80 °C oven for three days. Red bulk crystals formed during the reaction. Based on the amount of Ti added, the yield is 48%. Anal. Calcd. (%; MW = 4725.97): Ti, 14.2; C, 49.8; H, 3.6. Found (%): Ti, 13.8; C, 49.6; H, 3.9.

Synthesis of $Cs_2Ti_{14}O_{12}(Sal)_{10}(HSal)_{14}(C_3H_6O)_2\cdot 2(CH_3CN)\cdot 6(C_3H_6O)$ (denoted as $Ti_{14}Cs_2$)

Salicylic acid (1.65 g, 12 mmol) and cesium acetate (0.19 g, 1 mmol) were added to a 4.0 mL acetonitrile and acetone (1:1 v/v) mixture in a 20 mL vial. During stirring, acetic acid (0.5 mL, 8.75 mol) and $Ti(O^iPr)_4$ (0.92 mL, 3 mmol) were added dropwise to afford a red solution. After stirring for an hour, the vial was sealed and heated in an oven at 80 °C for three days. Red lumpy crystals formed during the reaction. Based on the amount of Ti added, the yield is 65%. Anal. Calcd. (%; MW = 4955.70): Ti, 13.5; Cs, 5.4; C, 47.5; H, 3.3. Found (%): Ti, 13.2; Cs, 5.3; C, 47.8; H, 3.2.

Single crystal X−ray diffraction (SC−XRD)

Crystallographic data for $Ti_{14}(NH_4)_2$: formula, $Ti_{14}O_{92}C_{196}N_4H_{172}$; moiety formula, $(NH_4)_2Ti_{14}O_{12}(Sal)_{10}(HSal)_{14}(C_3H_6O)_2{\cdot}2(CH_3CN){\cdot}6(C_3H_6O)$; calculated MW =4725.97 g mol^{-1}; T = 173 K; crystal system, triclinic ; space group, P-1 ; a = 16.8649(4) Å, b = 18.7159(4) Å, c = 18.7422(5) Å, α = 119.555(2)°, β = 100.296(2)°, γ = 91.512(2)°, V = 5017.7(2) $Å^3$; Z = 1; ρ_{cald} = 1.564 g cm^{-3} ; μ = 5.361 mm^{-1}; F(000) = 2420.0; $2\theta_{max}$ = 153.346; 56994 reflections; 19808 independent reflections (R_{int} = 0.0710); R_1 = 0.0607, wR_2 = 0.1609 for final R indexes [I > = 2σ (I)]; R_1 = 0.0762; wR_2 = 0.1685 for all reflections; data/restraints/parameters = 19808/2/1351; GOOF = 1.084 for all reflections; max/min residual electron density, 2.30/-0.73 e $Å^{-3}$. The crystallographic data have been deposited as CCDC number 2324223.

Crystallographic data for $Ti_{14}Cs_2$: formula, $Ti_{14}Cs_2O_{92}C_{196}H_{164}N_2$; moiety formula, $Cs_2Ti_{14}O_{12}(Sal)_{10}(HSal)_{14}(C_3H_6O)_2{\cdot}2(CH_3CN){\cdot}6(C_3H_6O)$; calculated MW = 4955.70 g mol^{-1}; T = 173 K; crystal system, triclinic; space group, P-1; a = 16.9180(3) Å, b = 18.7743(3) Å, c = 18.7972(3) Å; α = 119.575(2)°, β = 100.097(1)°, γ = 91.7900(10)°; V = 5063.54(17) $Å^3$; Z = 1; ρ_{cald} = 1.625 g cm^{-3} ; μ = 8.070 mm^{-1}; F(000) = 2508.0; $2\theta_{max}$ = 153.216; 58483 reflections; 20017 independent reflections (R_{int} = 0.0631); R_1 = 0.0479, wR_2 = 0.1252 for final R indexes [I > = 2σ (I)]; R_1 = 0.0583; wR_2 = 0.1314 for all reflections; data/restraints/parameters = 20017/0/1318; GOOF = 1.049 for all reflections; max/min residual electron density, 1.92/-0.95 e $Å^{-3}$. The crystallographic data have been deposited as CCDC number 2324222.

Electrochemical and photoelectrochemical tests

To prepare the coating paste, 30 mg of the catalyst was dispersed in 1 mL of ethanol, followed by 40 μL of Nafion solution (5% aq, Sigma-Aldrich) and ultrasonacation for ca. 30 min. A piece of FTO glass (1 cm × 3 cm) was washed sequentially with acetone, deionized water, and ethanol under ultrasonication and then dried at room temperature to improve adhesion. The working electrode was prepared by applying a thin layer of the coating paste dispersion to the FTO glass and then air-drying it. A three-electrode system was used for the electrochemical and photoelectrochemical tests, with an Ag/AgCl electrode as the reference electrode and a Pt wire electrode as the counter electrode.

For the transient photocurrent measurements, the "amperometric i-t curve" method of the electrochemical workstation was used. The electrolyte was a 0.2 M Na_2SO_4 solution (1:10 v/v isopropanol water), in which isopropanol acted as the sacrificial reductant. The experiments were performed in air atmosphere. At a positive bias and under light irradiation, isopropanol quenched the photogenerated holes. The photogenerated electrons were removed by the bias, generating the anodic photocurrent.

The same electrolyte and electrodes were used for electrochemical impedance spectroscopy (EIS). The AC impedance method was used to perform the EIS studies in the frequency range of 0.01–10^6 Hz with an amplitude of 0.2 V as the open circuit potential. The experiments were performed in a dark, under-air atmosphere.

For the Mott-Schottky analysis, the experimental setup was the same, while the "Open Circuit Potential-TTime" method was used. The Mott-Schottky curves were measured at different frequencies in the dark. The experiments were performed in a dark, under-air atmosphere.

Cyclic voltammetry (CV) and differential pulse voltammetry (DPV) were conducted using a standard three-electrode system comprising a glassy carbon working electrode (diameter = 3 mm), a platinum wire counter electrode, and an silver wire reference electrode. The glassy carbon electrode was polished with 0.3 μm Al_2O_3

slurry, followed by thorough washing via ultrasonication to ensure a clean surface. The solution was prepared by dispersing 0.1 g of the cluster compound in acetonitrile under ultrasonication, and then filtered to remove any undissolved material. Tetrabutylammonium hexafluorophosphate ($TBAPF_6$) at a concentration of 0.1 M served as the electrolyte. Ferrocene was included as the internal redox standard at a concentration of 0.1 mg/mL. All measurements were performed under a nitrogen atmosphere to minimize interference. Polarization data were collected at a scan rate of 20 mV/s.

Procedure for guest exchange experiments

Exchange of NH_4^+ with Cs^+. 0.1 g (0.0211 mmol) of $Ti_{14}(NH_4)_2$ was dissolved in 3 mL of DMF in a 10 mL vial. A certain amount of CsCl was added, e.g., 0.0018 g (0.01055 mmol), 0.0036 g (0.0211 mmol), 0.0053 g (0.03165 mmol), 0.0071 g (0.0422 mmol), 0.011 g (0.0633 mmol), or 0.0142 g (0.0844 mmol). The dispersion was magnetically stirred for two days and then filtered. 0.8 mL of the filtrate was transferred to an NMR tube. A sealed capillary containing 0.5 M CsCl in D_2O was also inserted into the NMR tube. ^{133}Cs NMR was analyzed using fixed scan numbers. After NMR analysis, 100 mg of the filtrate was thoroughly dissolved in aqua regia and diluted 1000 times with water. The concentrations of Ti and Cs were analyzed using ICP-MS. Each experiment was repeated thrice, and the average values were reported.

Exchange of NH_4^+ with other cations. 1.0 mmol of solid MCl was added to 2.0 mL of 20 mM (0.189 g) $Ti_{14}(NH_4)_2$/DMF solution. The resultant solid-liquid mixture was stirred for 24 h and then filtered. 100 mg of the filtrate was dissolved in aqua regia and then diluted 1000 times with water. The sample was analyzed using ICP-MS to afford the concentration of M^+ in the 20 mM **Ti_{14}** solution (denoted as $[M^+]_1$). The saturated concentration of MCl in DMF was also measured ($[M^+]_2$). The concentration of the enclosed M^+ was calculated as $[M^+]_1 - [M^+]_2$.

Catalytic cycloaddition reactions of CO_2 with epoxide

The procedure is similar to our previsou studies.[4-7] 0.1 g of catalyst, 0.16 g (0.5 mmol) of cocatalyst TBAB, and 50 mg of biphenyl (as internal standard) were added into a 20 mL vial. The vial was sealed with a rubber stopper and purged with CO_2 for 10 min. A party balloon containing about 2.0 L of CO_2 was connected to the vial. Then, 3 mmol of epoxide was quickly injected using a syringe, and almost immediately, the dark reaction began. A water bath was used throughout the reaction to reduce the temperature change. Moreover, three high−power fans were installed to ensure the well ventilation of the lamp house. When performing a photocatalytic reaction, the vial was illuminated from the side. After the reaction, a small amount of the reaction liquid was withdrawn and extracted using a mixed solvent of water and ethyl acetate (1:1 v/v). The conversion and yield of the reaction were analyzed by GC.

Small−angle X−ray scattering (SAXS) analysis

SAXS analysis was performed using a laboratory SAXS/WAXS instrument (Xeuss 2.0, Xenocs, France) with Cu Kα radiation (1.54189 Å), two sets of motorized scatterless slits for beam collimation, and a Dectris Pilatus 1M pixel SAXS detector. The DMF solutions (e.g., 16.7 g L^{-1} of a TOC) and the background sample (DMF solvent) were examined for 30 min in a 1.5 mm quartz capillary tube. The data were reduced (integration and normalization) with the Foxtrot software package. The background deduction, data modeling, and pair distance distribution function (PDDF) were analyzed using the SAXS Data Analysis ATSAS 3.1.1 software. The crysol tool of ATSAS 3.1.1 was used to simulate the spectra of the TOCs.

DFT simulation

Theoretical investigations were performed with the hybrid B3LYP density functional in the Gaussian09 program. The Lanl2DZ pseudo-potential was applied for the metal atoms while 6-31G** basis set was used for the other atoms. The order of the computed bandgap energy in the work by Wright et al.,[8] which calculated the density of states (DOS) of four Co-doped TOCs, matched the findings of the experiments. Nevertheless, there

was never a significant difference between the observed and computed band gap energies. Their observations aligned with ours.

To determine the DOS, we employed three techniques. Initially, DFT calculations were performed simply using the crystallographic geometries, without any structural optimization. Secondly, TDDFT calculations were performed directly using the crystallographic geometries. Third, the DFT approach was used to determine the DOS once the structure had been optimized. The HOMO-LUMO gap calculation is displayed in the following table.

Method	bandgap energy of $Ti_{14}(NH_4)_2$	bandgap energy of $Ti_{14}Cs_2$
1	3.08 eV, 403 nm	3.05 eV, 407 nm
2	2.67 eV, 465 nm	2.64 eV, 468 nm
3	3.00 eV, 414 nm	2.94 eV, 421 nm

It is evident that Ti14Cs2's bandgap energy is smaller than what is theoretically predicted. The calculated difference between the two cluster compounds—that is, 5 nm vs. 70 nm—is substantially less than the experimental difference.

2. Supplementary data

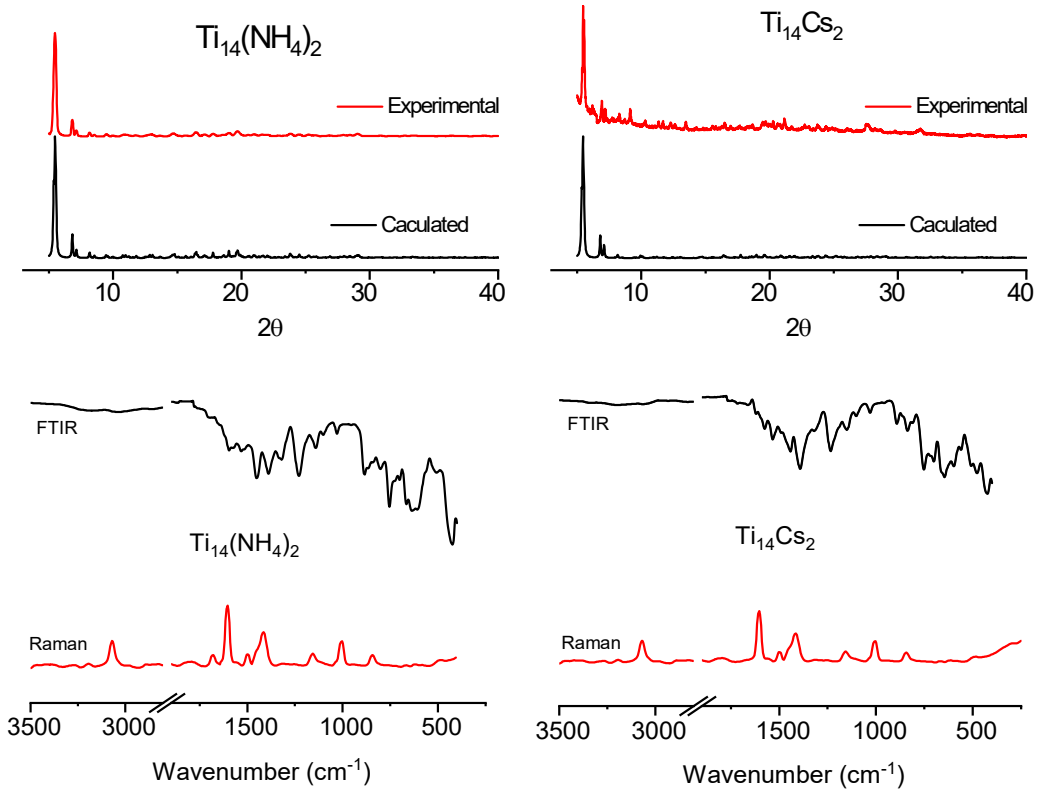

Figure S1. PXRD, FTIR, and Raman spectra $Ti_{14}(NH_4)_2$ and $Ti_{14}Cs_2$.

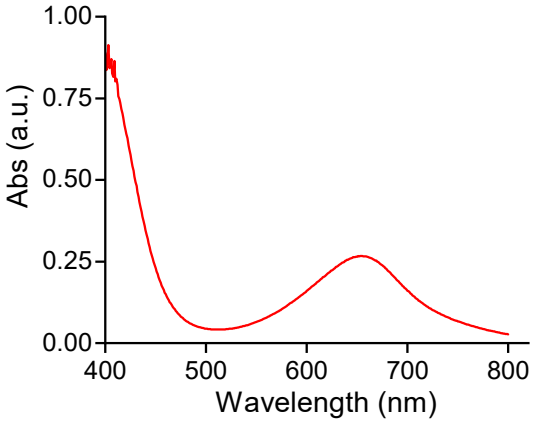

Figure S2. The UV-visible spectrum for determination of NH_4^+.

Description. Quantitative determination of NH_4^+ was performed using a chemical colorimetric method.[9] In detail, a 0.25 g mL^{-1} solution of $Ti_{14}(NH_4)_2$ in DMF was prepared. 2.0 mL of this solution was taken, adding a 2.0 mL solution containing 5 wt% salicylic acid, 1 M sodium hydroxide, and 5 wt% sodium citrate. Then, 1.0 mL of 0.05 M sodium hypochlorite solution and 0.2 mL of 1 wt% ferric nitrate were added. The solution turned green, and a precipitate formed rapidly. The precipitate was removed by filtration through a 0.22 μm membrane. The resultant filtrate was stood for 0.5 h and then analyzed using a UV-visible spectrophotometer. The peak at 660 nm was used to quantify the amount of NH_4^+ in $Ti_{14}(NH_4)_2$. Anhydrous ammonium acetate was used as the authentic standard to obtain the working curve. The results indicate that each $Ti_{14}(NH_4)_2$ molecule contains 2 NH_4^+ ions.

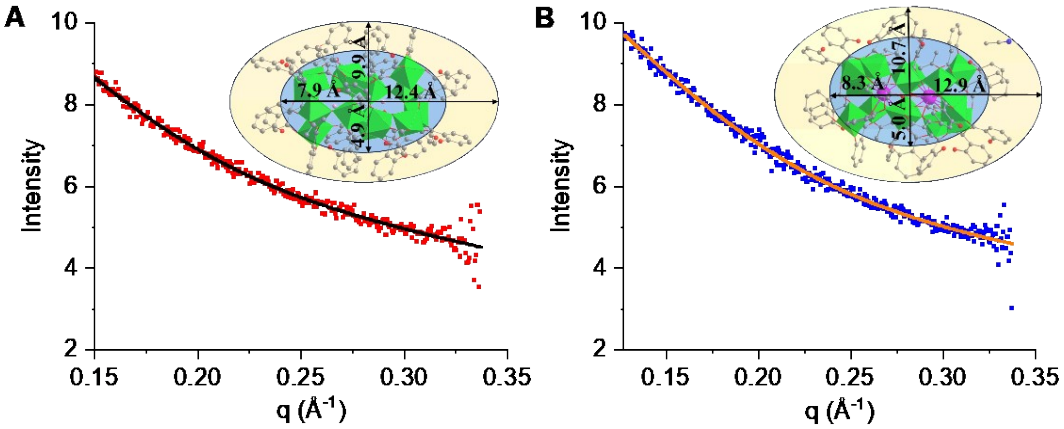

Figure S3. SAXS patterns of $Ti_{14}(NH_4)_2$ (**A**) and $Ti_{14}Cs_2$ (**B**) in DMF. Scatters, experimental data. Smooth curve, fitted curve. The inset shows the crystallographic dimension of the TOCs.

Discussion: The pair distance distribution function curve (PDDF) of $Ti_{14}(NH_4)_2$ shows a strong distribution in the low−r region with the peak maxima at 3.3 Å, followed by two smaller peaks at approximately 14 and 23.5 Å. The core structure of $Ti_{14}(NH_4)_2$, which has a high electron density, is responsible for the intense distribution of 0−9.7 Å. The second relatively small distribution of 9.7−19.7 Å is contributed by the core of $Ti_{14}(NH_4)_2$ and the ligands. The last distribution between 19.7 and 25 Å is exclusively ascribed to the coordinated ligands. Due to the identical molecular framework between $Ti_{14}Cs_2$ and $Ti_{14}(NH_4)_2$, their peak distributions in the PDDF curves are almost identical, but the radius of $Ti_{14}Cs_2$ is more significant than that of $Ti_{14}(NH_4)_2$. Notably, the PDDF curve matches well with the simulated one by the crystallographic structure. Overall, the SAXS analyses indicate that $Ti_{14}(NH_4)_2$ and $Ti_{14}Cs_2$ retain structural integrity after dissolving in DMF.

Table S1. The Ti-O bond lengths of $Ti_{14}(NH_4)_2$ and $Ti_{14}Cs_2$.

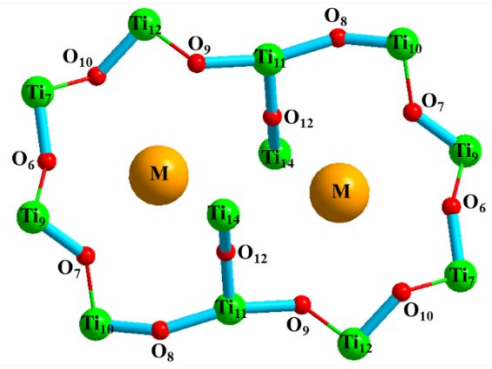

$Ti_{14}Cs_2$			$Ti_{14}(NH_4)_2$		
Atom 1	Atom 2	Bond length	Atom 1	Atom 2	Bond length
Ti_{11}	O_{12}	1.7428	Ti_{11}	O_{12}	1.7366
	O_8	1.9277		O_8	1.9249
	O_9	1.9331		O_9	1.9302
Ti_{10}	O_8	1.7426	Ti_{10}	O_8	1.7393
	O_7	1.8324		O_7	1.8439
Ti_{14}	O_{12}	1.939	Ti_{14}	O_{12}	1.9273
Ti_9	O_6	1.7887	Ti_9	O_6	1.795
	O_7	1.7991		O_7	1.7946
Ti_7	O_{10}	1.7682	Ti_7	O_{10}	1.7705
	O_6	1.8285		O_6	1.8187
Ti_{12}	O_9	1.7297	Ti_{12}	O_9	1.7349
	O_{10}	1.8764		O_{10}	1.8694

[a] Only the Ti-O bonds of the Ti-oxide framework are analyzed. Color scheme: green, Ti; red, O; gold, M^+. The thick blue bonds become longer after Cs^+ replaces NH_4^+. The thin two-color bonds become shorter or nearly unchanged after Cs^+ replaces NH_4^+.

Discussion: According to the crystallographic structures, most Ti-O bonds of the $Ti_{12}Cs_2$ framework are longer than those in $Ti_{14}(NH_4)_2$.

Table S2. Comparison of ^{133}Cs NMR of a few Cs^+–enclosing host-guest compounds

Compound	**Composition**	**Solvent**	**Standard**	**Chemical shift, ppm**	**Ref.**
$Ti_{14}Cs_2$	Ti, Cs, C, O, N, H	DMF	CsCl	9.64	This work
$Ti_{12}Cs$	Ti, Cs, C, O, N, H	DMF	CsCl	11.7	[10]
$Cs@Ti_{12}Ser_6$	Ti, Cs, C, O, Cl, H	H_2O	CsCl	116.4	[11]
$Cs@Ti_7Cr_{14}$	Ti, Cs, Cr, C, O, H	CH_2Cl_2	CsCl	-53.4	[6]
$CsH_7[Al_8(pdc)_8(OAc)_8O_4]$	Cs, Al, C, O, H	DMSO	$CsClO_4$	-26	[12]
$Cs_2(UO_2)(Si_2O_6)$	Cs, Si, C, O, H	H_2O	CsCl	136.5, 61.4, 54.3, −13.5	[13]

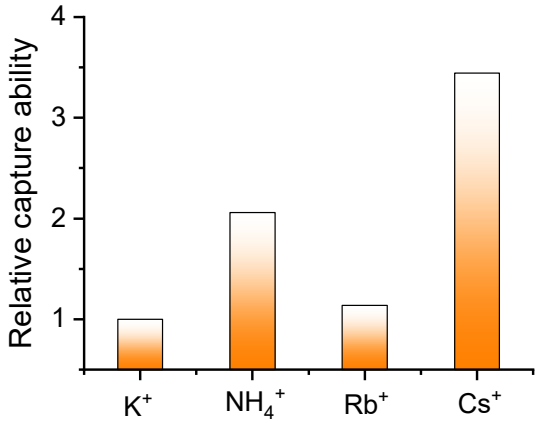

Figure S4. The relative ability of the **Ti_{14}** cage to capture M^+ (M^+ = Cs^+, Rb^+, NH_4^+, K^+).

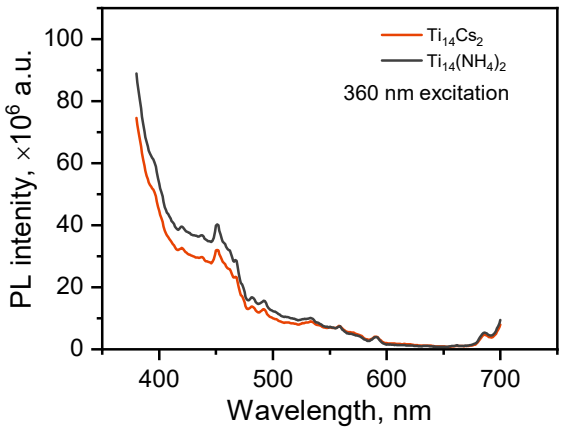

Figure S5. The photoluminescence spectra of $Ti_{14}Cs_2$ and $Ti_{14}(NH_4)_2$ using 360 nm excitation.

Using 360 nm excitation, we were able to obtain the photoluminescence spectra ranging from 400 to 700 nm. However, both cluster compounds only exhibit emission in 450-500 nm range, consistent with the spectra obtained using 300 nm excitation (Figure 5 in the main text). Moreover, the photoluminescence intensity of $Ti_{14}Cs_2$ is always weaker than that of $Ti_{14}(NH_4)_2$, indicating the recombination of charge carriers is slower.

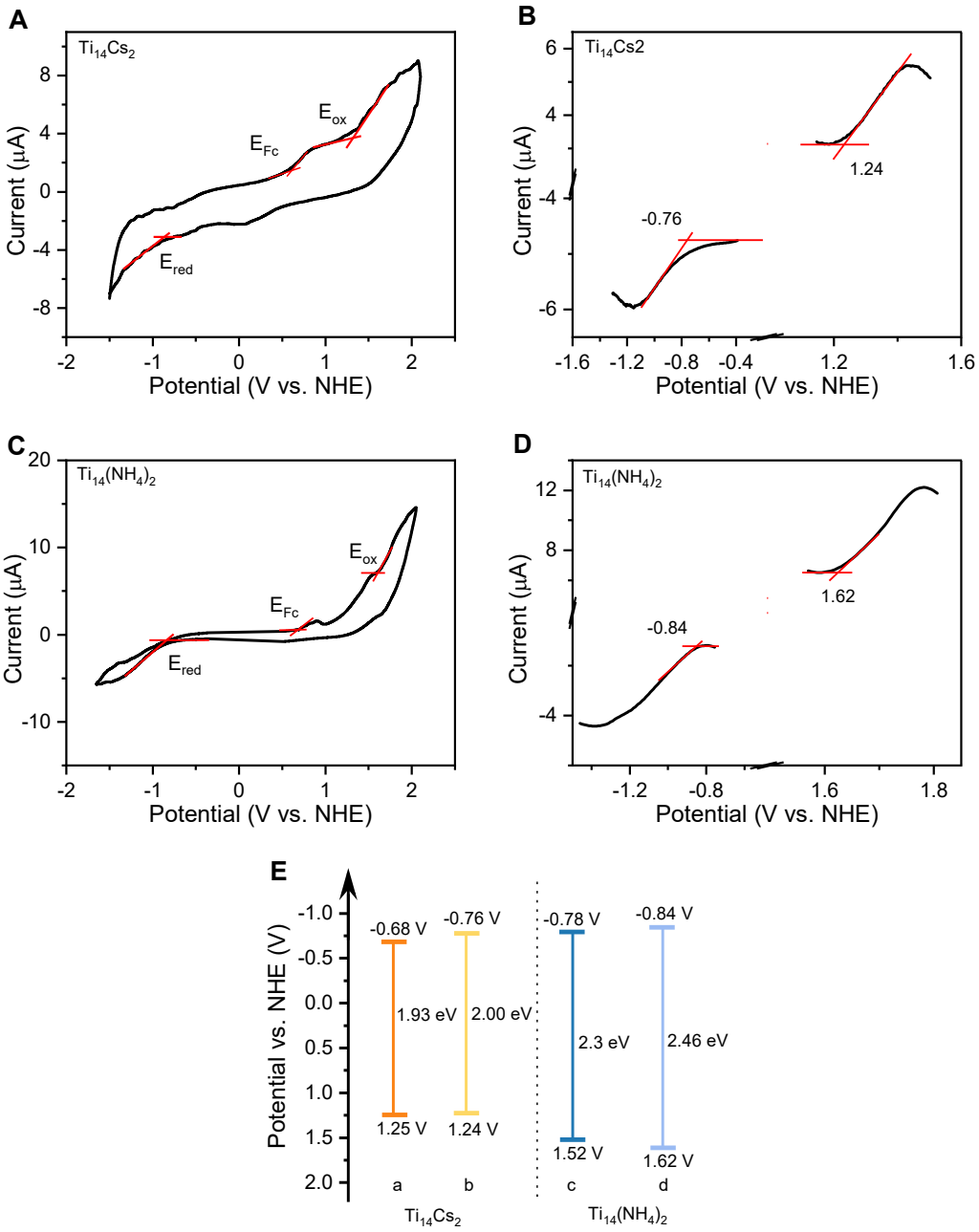

Figure S6. (**A**) CV and (**B**) DPW curves of $Ti_{14}Cs_2$. (**C**) CV and (**D**) DPW curves of $Ti_{14}(NH_4)_2$. The curves were obtained in N_2-saturated 0.1 M $TBAPF_6$ acetonitrile solution with ferrocene as the internal standard. (**E**) The schematic diagram of the band structures of $Ti_{14}Cs_2$ and $Ti_{14}(NH_4)_2$. (a) and (c) were obtained from Mott-Schottky and UV-vis DRS. (b) and (d) were obtained from electrochemical measurements.

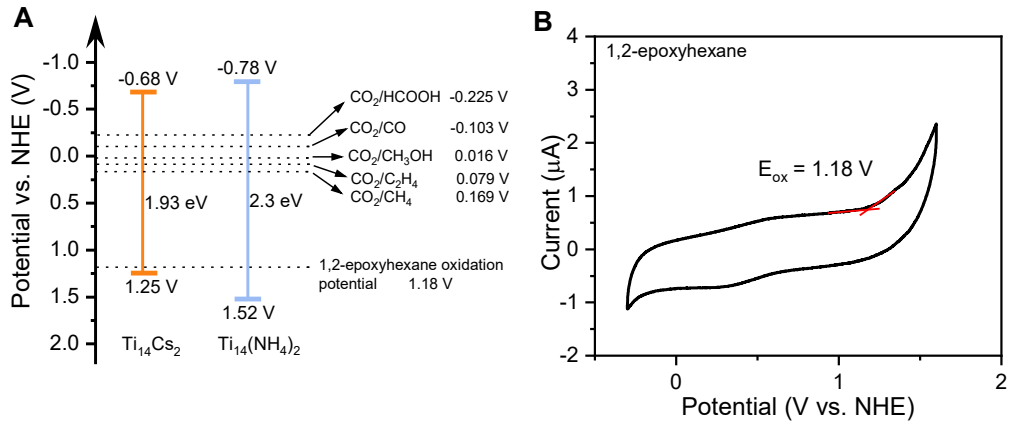

Figure S7. (**A**) The schematic electronic structure diagrams of $Ti_{14}(NH_4)_2$ and $Ti_{14}Cs_2$ and reactants. (**B**) The CV curve of 1,2-epoxyhexane.

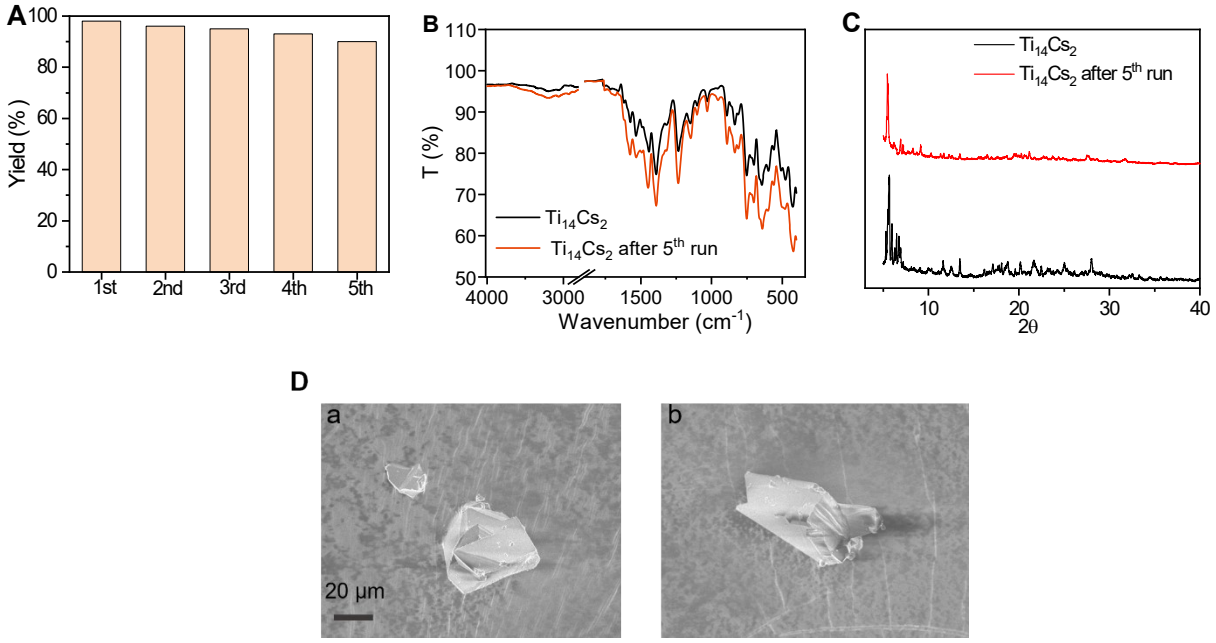

Figure S8. (**A**) The yields of the cycling experiments under the conditions: 1,2-epoxyhexane (3.0 mmol), $Ti_{14}Cs_2$ (100 mg), TBAB (0.5 mmol), CO_2 (1 bar), visible light, 20 °C. (**B**) FTIR, (**C**) PXRD and (**D**) SEM image before (a) and after reaction (b) of $Ti_{14}Cs_2$.

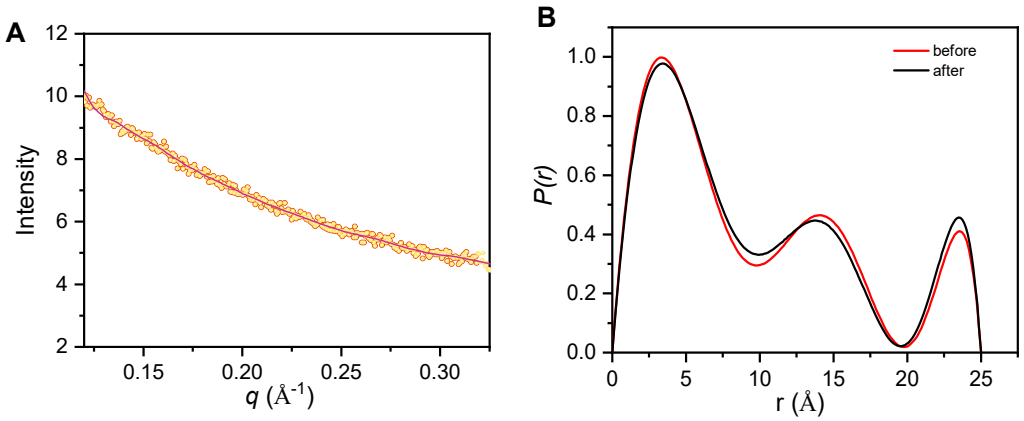

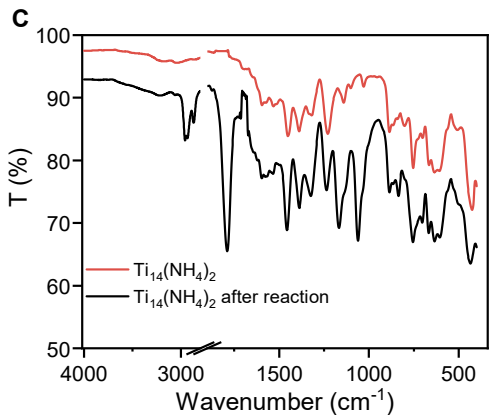

Figure S9. (A) The SAXS *I-q* spectra and (B) PDDF spectra of the reaction solution of the $Ti_{14}(NH_4)_2$ system before and after the cycloaddition reaction. The two curves are identical, suggesting $Ti_{14}(NH_4)_2$ remained stable. (C) The FTIR spectra of $Ti_{14}(NH_4)_2$ and the residue obtained by the rotary evaporation of the reaction solution after the cycloaddition reaction. All the peaks of $Ti_{14}(NH_4)_2$ remained intact, indicating $Ti_{14}(NH_4)_2$ remained intact. Conditions: 1,2-epoxyhexane (3.0 mmol), $Ti_{14}(NH_4)_2$ (100 mg), TBAB (0.5 mmol), CO_2 (1 bar), visible light, 20 °C. Therefore, $Ti_{14}(NH_4)_2$ remained stable during the cycloaddition reaction and was the genuine catalyst.

Estimation of the surface area of molecular $Ti_{14}(NH_4)_2$

$Ti_{14}(NH_4)_2$ resembles a centrally symmetric ellipsoidal shape, with a long axis of 25 Å and a short axis of 20 Å. Therefore, the surface area of an individual molecule is:

$$\frac{4}{3}\pi(ab+bc+ac) = 1466\ \text{Å}^2$$

The total surface area of 1 g of $Ti_{14}(NH_4)_2$ is calculated as follows:

$$\frac{\frac{1}{4726}\cdot 6.022\cdot 10^{23}\cdot 1797}{10^{20}} = 1868\ \text{m}^2$$

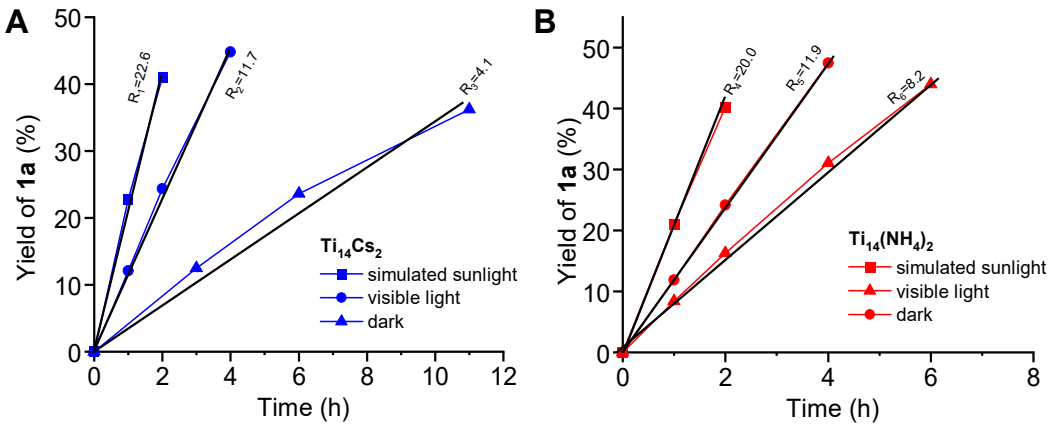

Figure S10. Calculations of the initial rates are shown in Figure 6A. (**A**) $Ti_{14}Cs_2$. (**B**) $Ti_{14}(NH_4)_2$.

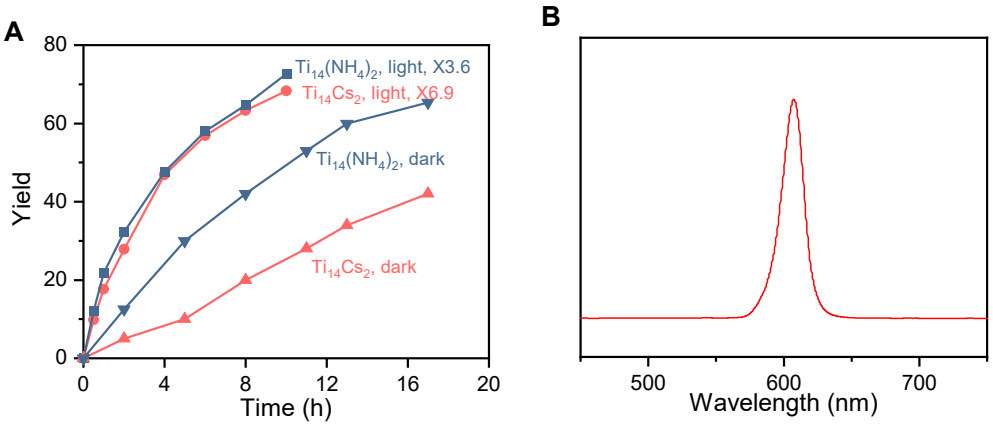

Figure S11. (**A**) Effects of 605 nm monochromatic LED (100 W) on the catalytic reactions. (**B**) The emission spectrum of the LED lamp.

Discussion. 605 nm accelerated the reactions in both catalytic systems. The enhancement factors are 3.6 and 6.9 for the $Ti_{14}(NH_4)_2$ and $Ti_{14}Cs_2$ systems, respectively. Both values are larger than those reported in Figure 6B (e.g., 2.4 and 5.5 for the $Ti_{14}(NH_4)_2$ and $Ti_{14}Cs_2$ systems under simulated sunlight irradiation). This is presumably attributable to the very high light intensity of the 605 nm LED. Nonetheless, the enhancement factor of $Ti_{14}Cs_2$ is almost twice of that of $Ti_{14}(NH_4)_2$ herein. This shows $Ti_{14}Cs_2$ has a better response to 605 nm light.

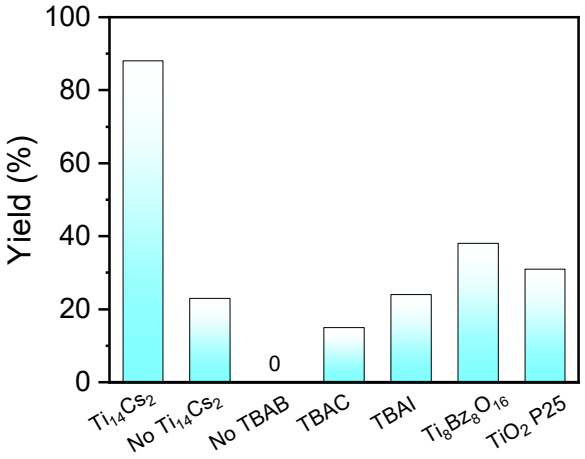

Figure S12. The yields of **1b** after 10 h of reaction in the control experiments. Only the changes from the standard conditions are indicated. Standard conditions: 1,2-epoxyhexane (3.0 mmol), $Ti_{14}Cs_2$ (100 mg), TBAB (0.5 mmol), CO_2 (1 bar), visible light, 50 °C, and 10 h.

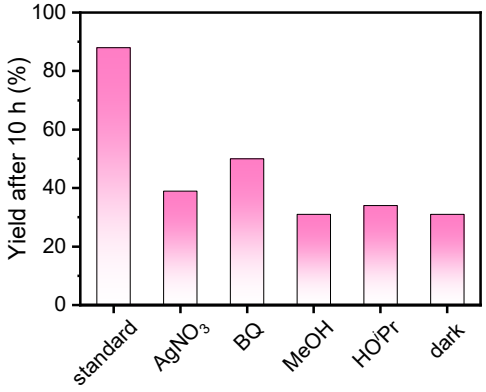

Figure S13. Effects of the quenchers on the yield. The amounts of the additives were typically 1 eq relative to 1,2-epoxyhexane. The additives were added together with the reactants prior to CO_2 purging. Standard conditions: 1,2-epoxyhexane (3.0 mmol), $Ti_{14}Cs_2$ (100 mg), TBAB (0.5 mmol), CO_2 (1 bar), visible light, 50 °C, and 10 h. "dark" means the experiment was performed following the standard conditions (no additive) but in the dark.

Discussion: Quenching experiments were conducted to verify the roles of photogenerated electrons (e^-) and holes (h^+). Common electron quenchers, such as $AgNO_3$ and 1,4-benzoquinone, and hole quenchers, like methanol (MeOH) and isopropanol (HO^{i}Pr), were utilized as additives under standard conditions. The conversion of **1a** and yield of **1b** significantly slowed down when these quenchers were introduced. The rates of the control experiments with the quenchers were similar to that of the "dark" reaction. This reasonably indicates that the additives quenched the photogenerated carriers. As long as either the photogenerated electrons or the photogenerated holes were quenched, the roles of visible light were diminished, and thereby only the Lewis-acid catalysis played a role in the cycloaddition reaction. Therefore, photogenerated electrons and holes played crucial roles in the cycloaddition reaction catalyzed by **$Ti_{14}Cs_2$** under solar−light irradiation.

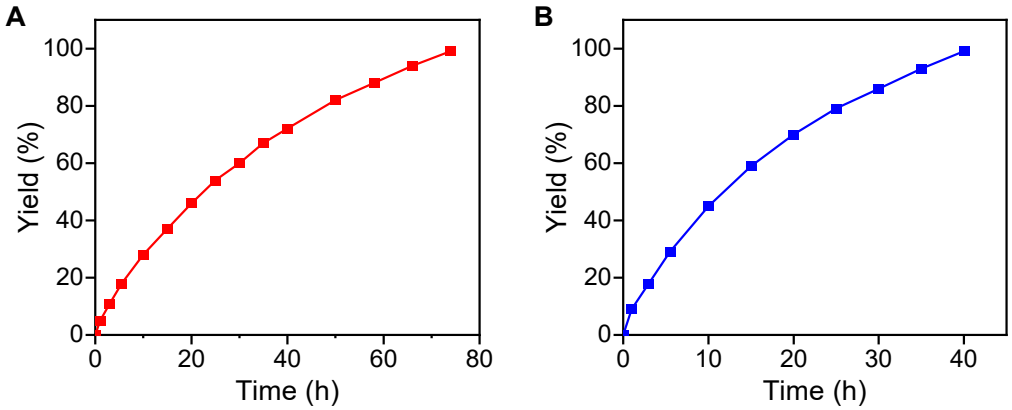

Figure S14. (**A**) The kinetics of the scale-up reaction. Conditions: 1,2-epoxyhexane (30 mmol), $Ti_{14}Cs_2$ (100 mg), TBAB (0.5 mmol), CO_2 (1 bar), biphenyl (0.05 g), 50 °C. (**B**) Reaction kinetics of the cycloaddition catalyzed by sunlight. The amount of 1,2-epoxyhexane was 3.0 mmol, while the other reaction conditions are identical to those of panel A.

Table S3. Comparison of the performances of the various catalysts used for the CO_2 cycloaddition to 1,2-epoxyhexane

Catalyst	Reaction conditions	Time, h	Conv., %	Yield, %	References
$Ti_{14}Cs_2$	Catalyst (50 mg); TBAB (0.5 mmol); epoxide (3 mmol); 1 atm CO_2; 20 ºC; simulated solar light.	23 h	100	>99	***This work***
$Ti_{14}Cs_2$	Catalyst (50 mg); TBAB (0.5 mmol); epoxide (3 mmol); 1 atm CO_2; 80 ºC; simulated solar light.	14 h	100	>99	***This work***
$Ti_{12}Cs$	Catalyst (50 mg); TBAB (0.5 mmol); epoxide (3 mmol); 1 atm CO_2; 50 ºC; visible light.	7.5 h	100	>99	*Dalton Trans.*, **2024**, *53*, 1989-1998
$Ti_{12}Pb_2$	Catalyst (50 mg); TBAB (0.5 mmol); epoxide (3 mmol); 1 atm CO_2; 20 ºC; visible light.	24 h	100	>99	*Dalton Trans.*, **2024**, *53,* 3666-3674
Ti_{14}	Catalyst (50 mg); TBAB (0.5 mmol); epoxide (3 mmol); 1 atm CO_2; 20 ºC; visible light.	30 h	100	>99	*Dalton Trans.*, **2024**, *53,* 3666-3674
Zn-NTTA	Catalyst (5 µmol); TBAB (0.3 mmol); epoxide (20 mmol); 10 bar CO_2; 100 ºC.	8 h	-	98.2	*ACS Appl. Mater. Interfaces,* **2016**, *8*, 31746-56.
Al–N_4–C	Catalyst (20 mmol); TBAB (0.8 mmol); epoxide (0.67 mmol); DMF; 1 bar CO_2; visible light.	60 h	-	80	*Adv. Mater.*, **2021**, *33*, 2103186.
MOF-801 (D)	Catalyst (0.6 mol%); TBAB (0.5 mol%); epoxide (19.2 mmol); 0.1 MPa CO_2; 80 °C.	15 h	92.4	92.4	*J. Mate. Chem. A*, **2022**, *10*, 10051–10061.
V_8-1	Catalyst (2 mol %); TBAB (0.5 mmol, 2.5 mol %); epoxide (28 mmol); CO_2 (0.5 Mpa); 70 °C.	16 h	-	>99	*J. Am. Chem. Soc.*, **2019**, *141*, 19487−19497.
Ni−TCPE1	Catalyst (10 µmol; based on Ni); epoxide (20 mmol); TBAB (0.3 mmol); CO_2 (1 MPa), 100	12 h	-	>99	*J. Am. Chem. Soc.*, **2015**, *137*,

	°C.				15066−15069.
Mn-MOF	Catalyst (10 mg); TBAB (0.028 mmol); epoxide (1.429 mmol); 1 bar CO_2; visible light; 80 °C.	24 h	-	90	*ACS Omega,* **2022**, *7*, 9958-9963.
PMo_{12}@Zr-Fc MOFs	catalyst (5 mg, 10.26 wt%); TBAB (0.25 mmol); epoxide (12.5 mmol); 1 atm CO_2; 80 °C; 900 rpm.	8 h	80	86.77	*Appl. Catal. B,* **2021**, *296*, 120329.
$CoPc/TiO_2$	Catalyst (100 mg); TBAB (0.1 mmol); epoxide (1.0 mmol); 1 bar CO_2; solvent (CH_3CN+MeOH); 20 W white cold LED, 25 °C.	24 h	96.7	94	*ACS Sustain. Chem. Eng.,* **2018**, *6*, 7799–7809.
Bi-PCN-224	Catalyst (30 mg); TBAB (0.5 mmol); epoxide (4.5 mmol); 1 bar CO_2; 300 W Xenon lamp.	6 h	>99	-	*ACS Catal.,* **2021,** *11*, 1988-1994.
$\{Cu_4[(C_{57}H_{32}N_{12})(COO)_8]\}_n$	Catalyst (0.2 mol%); TBAB (0.65 g, 10 mol %); CO_2 (1 atm); r.t.	48 h	-	96	*J. Am. Chem. Soc.,* **2016**, *138*, 2142−2145.
$Au_{19}Ag_4$(S-Adm)$_{15}$	Catalyst (5 mg); TBAB (10 mol%); epoxide (0.3 mmol); 3 ml solvent; 60 °C.	24 h	-	78	*Angew. Chem. Int. Ed.,* **2021**, *60*, 10573–10576.
IHEP-9	Catalyst (0.05 mmol); TBAB (0.5 mmol); epoxide (1 mmol); 1 bar CO_2; visible light; r.t.	12 h	-	>99	*Inorg. Chem.,* **2021**, *60*, 651-659.
Zr-MOF	Catalyst (30 mg); TBAB (0.5 mmol); epoxide (4.5 mmol); 1 bar CO_2; Xe lamp; r.t.	6 h	>99	-	*ACS Catal*. **2021**, *11*, 1988.
$Ti_{18}Bi_4$	Catalyst (100 mg); TBAB (0.5 mmol); epoxide (3.0 mmol); 1 bar CO_2; Xe lamp, r.t.	14 h	100	>99	*ACS Catal., **2022**, 12*, 8202−8213.
$BiNbO_4$/r-GO	Catalyst (50 mg); TBAB (9 mg); epoxide (100 µl); CO_2 (1.48 MPa); 353 K.	24 h	-	65	*ACS Sustain. Chem. Engin.,* **2020**, *8*, 12072-12079.
NUC-38Yb	Catalyst (0.5 mol %); TBAB (4 mol%); epoxide (20 mmol); CO_2 (1 atm); 60 °C.	10 h	-	96	*ACS Catal.,* **2021**, *11*, 14916−14925.

3. Reference

1. T. Frot, S. Cochet, G. Laurent, C. Sassoye, M. Popall, C. Sanchez and L. Rozes, $Ti_8O_8(OOCR)_{16}$, a New Family of Titanium–Oxo Clusters: Potential NBUs for Reticular Chemistry, *Eur. J. Inorg. Chem.*, 2010, **2010**, 5650-5659.
2. O. V. Dolomanov, L. J. Bourhis, R. J. Gildea, J. A. K. Howard and H. Puschmann, Olex2: A Complete Structure Solution, Refinement and Analysis Program, *J. Appl. Cryst.*, 2009, **42**, 339-341.
3. G. Zhang, C. Liu, D.-L. Long, L. Cronin, C.-H. Tung and Y. Wang, Water-Soluble Pentagonal-Prismatic Titanium-Oxo Clusters, *J. Am. Chem. Soc.*, 2016, **138**, 11097-11100.
4. A. Said, G. Chen, G. Zhang, D. Wang, Y. Liu, F. Gao, G. Wang, C.-H. Tung and Y. Wang, Enhancing the Photocatalytic Performance of a Rutile-Unit-Featuring Titanium-Oxide Cluster by Pb^{2+} Doping, *Dalton Trans.*, 2024, **53**, 3666-3674.

5. D. Wang, Y. Liu, G. Chen, F. Gao, G. Zhang, G. Wang, C.-H. Tung and Y. Wang, Ligation of Titanium-oxide and {Mo_2} Units for Solar CO_2 Storage, *Inorg. Chem.*, 2023, **62**, 21074–21082.
6. D. Wang, A. Said, Y. Liu, H. Niu, C. Liu, G. Wang, Z. Li, C.-H. Tung and Y. Wang, Cr–Ti Mixed Oxide Molecular Cages: Synthesis, Structure, Photoresponse, and Photocatalytic Properties, *Inorg. Chem.*, 2022, **61**, 14887-14898.
7. C. Y. Liu, H. H. Niu, D. X. Wang, C. Gao, A. Said, Y. S. Liu, G. Wang, C. H. Tung and Y. F. Wang, S-Scheme Bi-oxide/Ti-oxide Molecular Hybrid for Photocatalytic Cycloaddition of Carbon Dioxide to Epoxides, *ACS Catal.*, 2022, **12**, 8202-8213.
8. Y. Lv, J. Cheng, A. Steiner, L. Gan and D. S. Wright, Dipole-induced Band-gap Reduction in an Inorganic Cage, *Angew. Chem.*, 2014, **53**, 1934-1938.
9. M. Xu, F. Wu, Y. Zhang, Y. Yao, G. Zhu, X. Li, L. Chen, G. Jia, X. Wu, Y. Huang, P. Gao and W. Ye, Kinetically Matched C–N Coupling Toward Efficient Urea Electrosynthesis Enabled on Copper Single-atom Alloy, *Nat. Commun.*, 2023, **14**, 6994.
10. Y. Liu, G. Zhang, D. Wang, G. Chen, F. Gao, C.-H. Tung and Y. Wang, A Cryptand-like Ti-Coordination Compound with Visible-Light Photocatalytic Activity in CO_2 Storage, *Dalton Trans.*, 2024, **53**, 1989-1998.
11. G. Zhang, W. Li, C. Liu, J. Jia, C.-H. Tung and Y. Wang, Titanium-Oxide Host Clusters with Exchangeable Guests, *J. Am. Chem. Soc.*, 2018, **140**, 66-69.
12. S. Ilic, A. M. May, P. M. Usov, H. D. Cornell, B. Gibbons, P. Celis-Salazar, D. R. Cairnie, J. Alatis, C. Slebodnick and A. J. Morris, An Aluminum-Based Metal–Organic Cage for Cesium Capture, *Inorg.Chem.*, 2022, **61**, 6604-6611.
13. C.-S. Chen, R.-K. Chiang, H.-M. Kao and K.-H. Lii, High-Temperature, High-Pressure Hydrothermal Synthesis, Crystal Structure, and Solid-State NMR Spectroscopy of $Cs_2(UO_2)(Si_2O_6)$ and Variable-Temperature Powder X-ray Diffraction Study of the Hydrate Phase$Cs_2(UO_2)(Si_2O_6)\cdot 0.5H_2O$, *Inorg. Chem.*, 2005, **44**, 3914-3918.